IET Research Journals

Submission Template for IET Research Journal Papers

The Institution of Engineering and Technology

ISSN 1751-8644
doi: 0000000000
www.ietdl.org

Tip-Mold Micro-Contact Printing for Functionalization of Optical Microring Resonator

Nicola Peserico[1*], *Rossella Castagna*[1], *Laurent Bellieres*[2], *Manuel Rodrigo*[3], *Andrea Melloni*[1]

[1] *Dipartimento di Elettronica, Informazione e Bioingegneria, Politecnico di Milano, via G. Colombo 81, 20133, Milano, Italy*
[2] *Universitat Politecnica De Valencia, Camino De Vera, 46022 Valencia, Spain*
[3] *DAS Photonics SL, Calle Islas Canarias, 6 - 8, 46023 Valencia, Spain*
* *E-mail: nicola.peserico@polimi.it*

Abstract: We present an approach to functionalize optical microring resonators as hybridization platforms, using tip-mold reactive microcontact printing process. Derived from reactive micro-contact printing using an ad-hoc mold of Polydimethylsiloxane (PDMS), the method functionalizes single microring resonator with a target-specific capture agent. We report the functionalization of silicon nitride (SiN) $200\ \mu m$ diameter microring resonator with single-strand DNA and the hybridization detection of $100\ nM$ target analyte, while concurrently monitoring not-functionalized microring as a control sensor. Results show that the functionalization approach permits to address single microring resonators with mutual distance lower than $100\ \mu m$ with high precision, enabling a better integration of multiple spotting zones on the chip concerning traditional functionalization procedures.

1 Introduction

Molecular binding and hybridization process are widely studied techniques to investigate biological phenomena. Biosensors that can monitor such activities provide a valuable amount of information that can be used in clinical diagnosis, environmental monitoring and so on[1, 2]. Biosensors using label-free approach achieve faster results than traditional sensors due to a much simpler sample preparation[3]. Nevertheless, these sensors require control references close to the sensing points to avoid false positive signals, that are due to parasitic effects such as temperature variation, different analyte solution composition, or non-specific binding[4].
Photonics integrated circuits (PICs) are becoming one of the major candidates as the new label-free biosensors. When light is confined in a nanoscale structure, such as in a photonic waveguide, interactions between the light and the surrounding materials occur due to the evanescent optical field. The interactions induce a perturbation of the light properties that can be detected by optical circuits, typically interferometers exploited as biosensors, such as Mach-Zehnder interferometer[5], or resonators (e.g., microring resonators, Fabry-Pérot microcavities[6], photonic crystals[7] and Bragg gratings). Several reasons support this photonic biodetection technology out of all nanoscale structures based on light interaction with small quantities of analyte allowing the detection of pM quantities[8]. Moreover, PICs permit to integrate on the same chip a large number of sensing points, providing the multiplexing of different capture agents, a significant important feature in many diagnostic and sensing cases. These sensors have been successfully used to detect several different analytes, such as proteins[9], DNA[10, 11], cancer biomakers[12] and so on.
The functionalization of the waveguide has a large impact on the sensitivity of the biosensor and represents a crucial step in the realization of these sensors[13]. The functionalization is used to place target-specific capture agent (such as antibodies and DNA probes) over the waveguide core employing a biochemical protocol. Typical protocols consist of three main steps, silanization of the surface, activation of the reactive groups and probes immobilization[14], performed by immersion of the PIC in different solutions. The last step can be carried out with commercial microarray spotters with spot diameter that can go down to $100\ \mu m$. Multiplexing with inkjet spotter has been achieved for Silicon-on-Insulator PICs by J.T. Kirk et al.[15], where single $120\ \mu m$ diameter microring are spotted with high precision. However, all these methods require spotting solution volumes as large as hundreds of picoliters (pl) over the microring, an operation that limits the proximity between microrings.
Micro-contact printing (μCP) is a known method to pattern probes, by microlithography, over substrates to obtain precise geometries. The vast literature on the subject reports many applications of the soft lithography technique to biomolecules such as deposition of DNA[16], protein[17] and cells[18]. Pattern mold is inked with functional agents that are transferred to the surface by soft pressure: by using an ad-hoc material as the mold (e.g., Polydimethylsiloxane, PDMS), the higher affinity of probes with the surface than the one with the mold is exploited, allowing their transfer to the surface. The stable binding between the probes and the substrate required by hybridization platform can be achieved by Reactive micro-contact printing ($R\mu CP$) process. Introduced by Whiteside's group[19], $R\mu CP$ achieves the creation of a covalent probe immobilization exploiting the reactive nanoscale confinement of the soft-lithography. Wide and well-defined areas can be functionalized by this technique with the advantage of the ligation of the molecules to the surface to achieve a stable immobilization[20].

In this paper, we propose a straightforward and efficient $R\mu CP$ method to deposit single-strand DNA (ssDNA) probes over a photonic waveguide, using a tip with PDMS on it. We demonstrate this approach by experimentally deposit ssDNA over a $200\ \mu m$ diameter optical microring and monitoring the hybridization activity when complementary strands of DNA flow over. Since double-strand DNA (dsDNA) has a different refractive index (≈ 1.54) compared with the ssDNA's refractive index (≈ 1.46)[21], a shift of the resonance wavelength of the microring is recorded during hybridization experiments. A graphical representation of the functionalization steps is shown in fig. 1. The low cost of materials required for the functionalization, the high precision, and the low risk to contaminate adjacent waveguides are essential features of this method.
The paper is organized in 4 sections: after the introduction, a description of the experimental methods is presented in section 2, while experimental results are listed in section 3. Section 4 is dedicated to the conclusions.

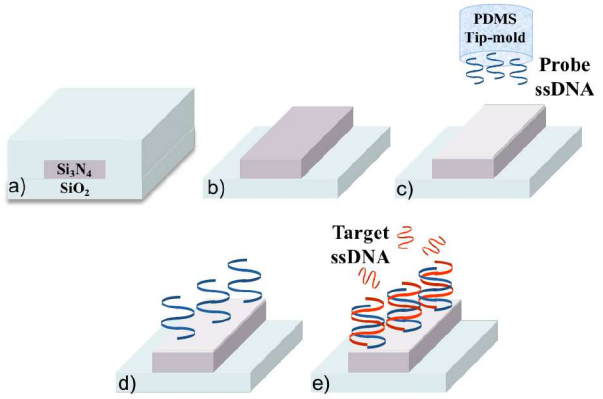

Fig. 1: (a) Waveguide cross-section of the reference microring. (b) Waveguide cross-section of the control microring. (c-e) Graphical representation of the various functionalization steps: ssDNA are applied over the waveguide by PDMS tip-mold $R\mu CP$, so that the hybridization with complementary target ssDNA can occur over the waveguide and be detected by read-out system.

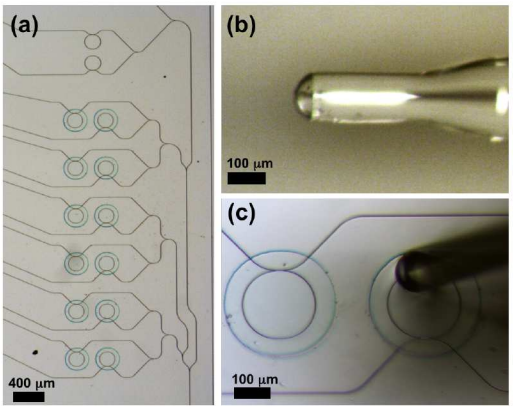

Fig. 2: (a) Optical image of the microring array. Microrings at the top serve as the temperature reference, while all the others are the microrings with cladding removed, that can be either used as control or sensors. (b) Fiber tip with a solid PDMS cladding. (c) Example of functionalization with PDMS on fiber. It is possible to address precise portions of the waveguide, without affecting other microrings.

2 Experimental Methods

To demonstrate our proposal technique, a PIC composed by several microring resonators is functionalized to detect the presence of complementary ssDNA in solution. This section presents the design and the realization of the PIC and its functionalization by $R\mu CP$, using our fiber-mold and ssDNA sequences.

2.1 Photonic Chip Design and Realization

Silicon Nitride waveguides with a rectangular shape (dimension $1200\,nm$ wide and $300\,nm$ thick) have been used. Due to the shallow thickness, the fundamental TE mode has a large evanescent field toward upper cladding, while a low curvature radiation loss is guaranteed.
The PIC, showed in fig. 2a, is composed by 12 uncovered all-pass optical microrings and 2 buried ones. The buried microrings use the waveguide shown in fig. 1a and are used as temperature references, whereas the uncover ones can be utilized either as control microrings (with no functionalization, fig. 1b) or as sensor microrings (functionalized, fig. 1c). Each microring has input and through ports connected with grating couplers for coupling the input and output light signal. All the experiments have been performed at a wavelength around $1550\,nm$, allowing to use technologies and instrumentation commonly used in the telecommunication field. The spectra of the microrings are taken by using a tunable laser with linewidth below 1 MHz, and an optical spectrum analyzer, allowing a resolution of 2 pm. During hybridization experiment, wavelength span range is limited to one Free Spectrum Range to be able to acquire as many spectra as possible. Cross-correlation between time-shift spectra of the same microring is used to compute the wavelength shift in time. The details of the fabrication are given in section 7.1.

2.2 Chip Functionalization

Exposed waveguides are functionalized by process of surface silanization and reactive groups activation. The first step of the protocol consists in the washing of the sample chip with a solution of 1% Nitric Acid in D.I. water, rinsed in water and dried with nitrogen flow. Silanization, the process that links alkoxysilane molecules to the chip surface, is carried out by immersing the chip overnight in a solution of 2% v/v APTES in ethanol, rinsed with isopropanol and water, followed by an overnight dry in an oven at $110^o\,C$. Next, carboxylic acid functionalization surface is obtained by immersion of the sample in succinic anhydride solution ($0.1\ M$ in dimethyl sulfoxide) for 8 hours, following by rinsing in isopropanol and drying by a nitrogen gas flux[22]. Just before the deposition of probes, interested area was covered by a solution of $1\ mg/ml$ EDC in D.I. water for 45 min. The chip is hence dried by removing the EDC solution and immediately used for printing the ssDNA probes.

2.3 Tip-Mold Preparation

A short section of standard optical fiber is used as tip-mold for the $R\mu CP$: this choice combines the versatility of the mold preparation with the high compatibility between fiber and PDMS. Moreover, fiber has a flat surface at the end due to cleaving process and permits to cover part of the microring area (depending on the microring diameter). The small cross-section of a standard optical fiber ($125\ \mu m$ diameter) and the accuracy of positioning over the waveguide are also important features. In a beaker PDMS is prepared by mixing its basic components with 10:1 w/w ratio between prepolymer and crosslinker and processed in a vacuum chamber for bubbling. A section of single-mode fiber has its buffer and jacket removed, and the end is cleaved to have a flat surface. Then it is cleaned with isopropanol and nitrogen flow, and dipped in the PDMS, so that a small quantity remains over the tip of the fiber (as shown in fig. 2b). The control of immersion and emersion velocity of the tip in the PDMS solution ensures a uniform coverage with a good repeatability. The fiber is then placed in an oven at $65^o\,C$ for 2 hours to increase the curing reaction kinetics of PDMS. Before the immersion in the solution containing the DNA probes, PDMS is immersed in a solution of hydrochloric acid, hydrogen peroxide and D.I. water (2.5ml-1.5ml-6ml, respectively) for 30 minutes. This step decreases the hydrophobicity of PDMS surface and increases the affinity of the siloxane stamp with an aqueous solution, which assures a better inking with the probes when is used (details are provided by R. Castagna et al. in Ref. [20]).

2.4 Probes and Hybridization

The tip-mold fiber covered by PDMS is immersed in a solution of $5\ \mu M$ of amino modified DNA probe sequence (ssDNA1, as reported in Table 1) for 5 minutes. After that, fiber is placed on a micrometric positioner and moved above the selected microring. The fiber is pressed over the interested ring waveguide for 45 minutes in a controlled environment, with 50% humidity, as shown in fig. 2c. Being the ring diameter $200\ \mu m$, only the 25% of the ring length is functionalized. This is sufficient to reach a good sensitivity and

Table 1 ssDNA sequences used as probe and target strands.

Name	Sequence
Probe: ssDNA1	$5'-NH_2-GCC\,CAC\,CTA\,TAA\,GGT\,AAA\,AGT\,GA-3'$
Target: ssDNA2	$5'-Cy3-TC\,ACT\,TT\,ACC\,T\,AT\,AGG\,TGG\,GC-3'$

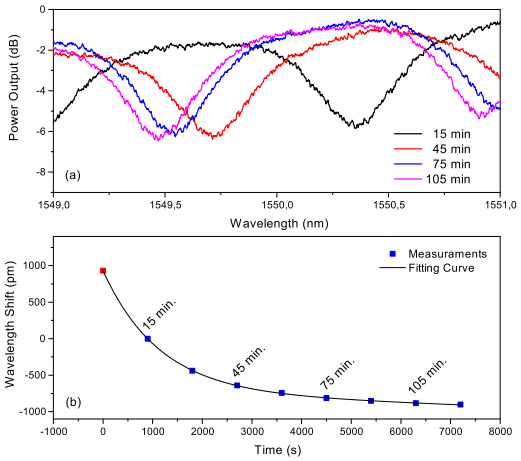

Fig. 3: (a) Normalized spectra acquired during hybridization experiment. Spectra are taken every 15 minutes and show a wide blue shift, while the shape of the notch at the resonances frequency does not change. (b) Resonance shift versus time. Experimental measurements acquired every 15 minutes fitted by a linear combination of Langmuir binding model due to specific binding and a linear law due to not specific binding and temperature shift. Shift at time 0 (red point) is extrapolated from the fitting.

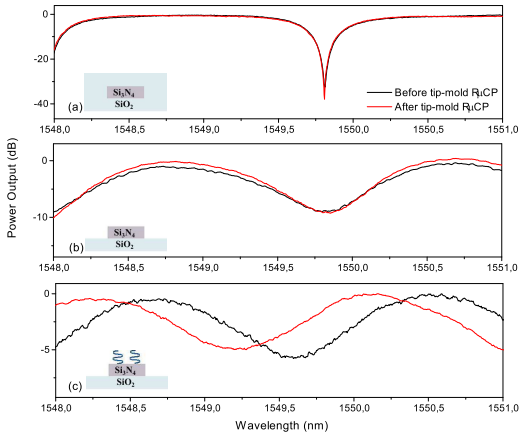

Fig. 4: Spectra of three different microrings taken before (black spectra) and after (red spectra) the $R\mu CP$. (a) Reference buried microring. Due to the thick cladding that covers the microring, the functionalization does not affect the spectral response. It is used only as a temperature reference. (b) Not-functionalized control microring is adjacent to the sensing microring. (c) Spectra of the sensing microring with DNA probes functionalization.

if needed can be repeated to cover the entire microring. The chip is then washed with saline buffer solution (SSC 0.1 in D.I. water). Binding with full match complementary target strand ssDNA2 (see Table 1) is performed according to the procedure reported in the literature[20]. Briefly, a solution ($2X$ SSC,0.1% SDS, 0.2mg/ml BSA in D.I. water) with a given concentration of ssDNA2 is flowed over the chip, while Peltier plate heats the chip to $47^o\,C$, a temperature that promotes the hybridization between DNA strands. In this condition, tunable laser and optical spectrum analyzer are used to capture spectra of several microrings during the two hours of the binding process[23].

3 Results and Discussion

This section presents experimental results. First of all, a hybridization test using classical drop casting is performed and used as a comparison with the presented fiber tip-mold $R\mu CP$ functionalization hybridization procedure. All the steps of the functionalization are presented, in particular showing the change in the microring effective refractive index due to the probes immobilization. This section lasts with the experimental hybridization with complementary ssDNA that proves the effectiveness of the method.

3.1 Drop Casting Reference Hybridization Test

As a reference for the tip-mold $R\mu CP$ procedure, hybridization test with probes placed by solution drops is considered. A drop of 100 μl of a solution containing 5 μM of ssDNA1 is poured out to cover several microrings for 45 minutes at room temperature. After washing with saline buffer solution, the sample is placed over the Peltier plate at $47^o\,C$ and covered by the hybridization solution containing 1 μM of ssDNA2. The spectra of a microring, acquired every 15 minutes, are shown in fig 3a. Due to the setup limitation and temperature range reached by the sample, spectrum at time 0 is not available. The measured temporal shift $\psi(t)$ of the microring resonance follows the Langmuir binding model[24], together with a linear shift due to parasitic effects such as temperature variation and non-specific binding. The Langmuir model can be expressed as $\psi(t) = \psi_\infty\{1-\exp(-K_1\rho_A t)\}$, where ψ_∞ is the shift at the time of saturation, ρ_A $[M]$ is the concentration of the analyte over the chip and K_1 $[M^{-1}s^{-1}]$ is the association constant. The fitted curve ($R^2 = 0.996$) returns a rate of the binding of $8.75\cdot10^{-4}$ s^{-1}, so K_1 can be estimated as 875 $M^{-1}s^{-1}$, while linear drift has a slope of 0.024 pm/s. The linear drift is compatible with a shift of about $21^o\,C$ that is the difference between the temperature of the hybridization solution (room temperature $25^o\,C$) and the temperature of the microchip ($47^o\,C$). The amplitude of the exponential contribution ψ_∞ results of 1.8 nm after 2 hours.

3.2 Hybridization Platform Functionalization

In this section, the waveguide functionalization performed using tip-mold $R\mu CP$ is presented. In figure 4 the spectra of three microrings taken before and after the $R\mu CP$ are shown. In fig. 4a the spectrum of the buried microring is reported. The resonance of the microring is not affected by the functionalization due to the thick uppercladding (2 μm of Silica). Only the printed microring shows a significant spectral shift (fig. 4c) due to the probe binding to the surface, while the control microring shows no significant shifts (fig. 4b). This confirms that DNA probe deposition is performed correctly. Just 100 μm spaces control and sensing microrings, but no mutual contamination occurs. The resonance shift induced by the DNA probes is quantified at 300 pm. A control experiment of the $R\mu CP$ without any DNA strand is performed on a separate microring to verify the absence of wavelength shifts due to mechanical damage or contamination of the waveguide.
The quality of the coating reveals to be quite reproducible for different trials, even if optimization of the method is not performed. For example, PDMS covers the tip with a hemisphere shape, reducing the area that contacts the waveguide. In the case of microrings with a diameter smaller than a standard optical fiber, tapered on lensed

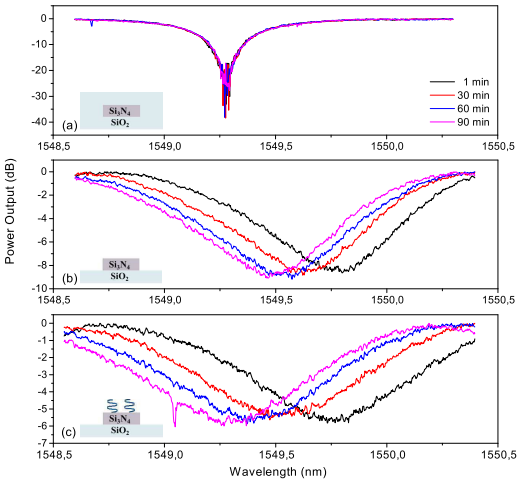

Fig. 5: Optical microring spectra acquired during target binding experiment. (a) Reference buried microring. (b) Control microring not-functionalized. (c) Sensing microring: the large shifts compared to the control microring can be attributed to target hybridization activity.

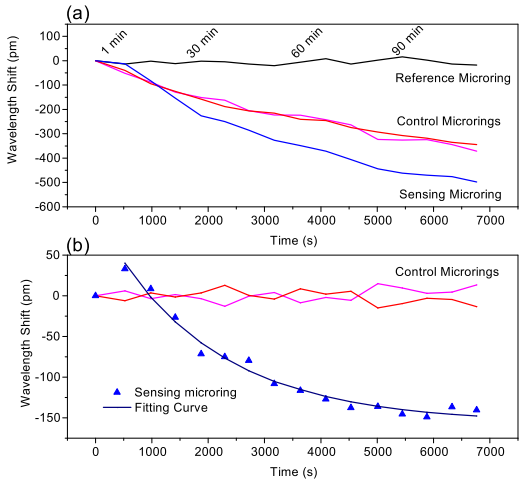

Fig. 6: Wavelength shift induced during target binding experiment. (a) Wavelength shifts of the resonance of four different microrings: reference microring used for temperature standard, two control microrings and the functionalized one. (b) The average of the two not-functionalize microrings is subtracted from the last three of the upper plot. This difference of shifts indicates the correct binding of functionalized microring.

fibers can be used, together with different tip materials, whose compatibility with PDMS has to be verified.
The desired position of the fiber over the ring is achieved by using a micropositioner widely use in photonics laboratories. We used a Thorlabs 3-Axis NanoMax Stage MAX300, allowing a position accuracy of 1 μm. Accuracy is also improved by the possibility of a visual inspection with a microscope, that is permitted due to the dry condition at which the functionalization is made. Stability of the fiber over the chip is the results of the stability of the optical bench.

3.3 Target Hybridization Experiment

Functionalized microrings have been used in the hybridization tests with 100 nM target ssDNA2, and experimental results are here reported. The experiments are performed using a microfluidic channel, where the solution is injected with a syringe. In fig. 5 the spectra of a reference, control, and sensing microring are shown. A small frequency shift is also observed on the control ring, similar to the linear shift described in the Sec. 3.1, with a slope of 0.026 pm/s.
In fig. 6 wavelength shifts occurring during target binding experiment are shown. The reference buried microring permits to monitoring the temperature fluctuation of the Peltier module during the experiment, evaluated within $\pm 1^o\,C$. The spectral responses of two control microrings show the linear drift due to different causes, such as temperature difference between solution and microchip, and non-specific binding. The sensing microring presents a larger shift attributed to hybridization process. The linear drift due to temperature is common to the control microrings and the sensing microring and can be subtracted obtaining the result shown in fig. 6b. The exponential trend appears clearly on the functionalized microring, with a shift of about 180 pm, as the target ssDNA is less concentrated in the hybridization solution. The exponential fitting curve is computed and plotted ($R^2 = 0.987$), with the binding rate of $4.35 \cdot 10^{-4}\ s^{-1}$, which returns an association constant of $K_1 = 1914\ M^{-1}s^{-1}$. This last parameter is comparable with values reported in the literature[25] and can be increased if functionalization optimization is performed.

4 Conclusion

In this paper, we propose a method for the selective functionalization of optical waveguides using tip-mold $R\mu CP$. We describe the protocol to functionalize the waveguides of microring resonators and their use as hybridization platforms. We experimentally demonstrate the functionalization method by monitoring hybridization of 100 nM of complementary ssDNA with a differential shift of 180 pm, that match with the Langmuir exponential model. The functionalization method allows using near microrings as control reference to count for temperature variation, the composition of the solution, and non-specific binding.
With the proposed method, the multiplexing can be easily implemented by multiple tip-molds with different probes. Moreover, various sizes of tip diameter can be used in other to match the dimension of the microrings or the waveguide, so that the density of probes near the sensitive zone can be increased. Multiplexing and flexibility in functionalization procedures are key-factor for the photonic biosensors technologies and we expect that the proposed technique could reduce the cost and increase the reliability of biosensors. The flexibility of the method would ultimately improve the limit of detection of optical biosensors by increasing the number of probes in the sensing area (so only over the waveguide) and correspondingly reducing the probes in the blind area of the sensor. Specific tips with ad-hoc shapes can be proposed in the future.

5 Acknowledgments

The authors thank M. Chiari for the supply of the DNA strands and C. Somaschini, G. Iseni, L. Livietti, and M. Leone of Polifab for their skillful technical support. This work was mainly performed at Polifab [www.polifab.polimi.it], the micro- and nanofabrication facility of Politecnico di Milano.
This work was partially funded by Regione Lombardia and Fondazione Cariplo via the project n. 2013-1760 "ESCHILO-Early Stage Cancer diagnosis via Highly sensitive Lab-On-chip multitarget systems" and by EDA via the project BIOTYPE (Contract identifier: A-1152-RT-GP).

6 References

6.1 Journal articles

1 S. U. Senveli and O. Tigli, Nanobiotechnology, IET 7(1), 7-21 (2013).
2 D. Erickson, S. Mandal, A.H. Yang, and B. Cordovez, Microfluidics and nanofluidics 4(1-2), 33-52 (2008).
3 H. K. Hunt and A. M. Armani, Nanoscale 2(9), 1544-1559 (2010).
4 D.-X. Xu, M. Vachon, A. Densmore, R. Ma , S. Janz, A. Delâge, J. Lapointe, P. Cheben, J. H. Schmid, E. Post, Sonia Messaoudène, Jean-Marc Fédéli, Opt. Express 18(22), 22867-22879 (2010).
5 K. Zinoviev, L.G. Carrascosa, J. Sánchez del Río,B. Sepúlveda, C. Domínguez, L.M. Lechuga, Advances in Optical Technologies (2008).

6 A. M. Armani, R. P. Kulkarni, S. E. Fraser, R. C. Flagan, and K. J. Vahala, Science 317(5839), 783-787 (2007).
7 S. Chakravarty, Y. Zou, W. C. Lai, and R. T. Chen, Biosensors and Bioelectronics 38(1), 170-176 (2012).
8 M. C. Estevez, M. Alvarez, and L. M. Lechuga, Laser & Photonics Reviews 6(4), 463-487 (2012).
9 F. Vollmer, D. Braun, A. Libchaber, M. Khoshsima, I. Teraoka, and S. Arnold, Applied Physics Letters 80(21), 4057-4059 (2002).
10 A. J. Qavi and R. C. Bailey, Angewandte Chemie International Edition 49(27), 4608-4611 (2010).
11 J.S. del Río, T. Steylaerts, O. Henry, P. Bienstman, T. Stakenborg, W. Van Roy and C. O'Sullivan, Biosensors and Bioelectronics 73, 130-137 (2015).
12 A.L.Washburn, M.S.Luchansky, A.L.Bowman and R.C.Bailey, Analytical chemistry 82(1), 69-72 (2009).
13 S. Hu, Y. Zhao, K. Qin, S. T. Retterer, I. I. Kravchenko and S. M. Weiss, ACS Photonics 1(7), 590-597 (2014).
14 J. Kim, J. Cho, P. M. Seidler, N. E. Kurland, and V. K. Yadavalli, Langmuir 26(4), 2599-2608 (2010).
15 J. T. Kirk, G. E. Fridley, J. W. Chamberlain, E. D. Christensen, M. Hochberg, and D. M. Ratner, Lab Chip 11, 1372- 1377 (2011).
16 S.A. Lange, V. Benes, D.P. Kern, J.H. Hörber and A. Bernard, Analytical chemistry 76(6), 1641-1647 (2004).
17 S.A. Ruiz and C.S. Chen, Soft Matter 3(2), 168-177 (2007).
18 D. Tian, Y. Song, and L. Jiang, Chemical Society Reviews 42(12), 5184-5209 (2013).
19 L. Yan, X. M. Zhao, and G. M. Whitesides, Journal of the American Chemical Society 120(24), 6179-6180 (1998).
20 R. Castagna, A. Bertucci, E. A. Prasetyanto, M. Monticelli, D. V. Conca, M. Massetti, P. P. Sharma, F. Damin, M. Chiari, L. D. Cola, and R. Bertacco, Langmuir 32(13), 3308-3313 (2016).
21 S.Elhadj, G.Singh and R.F.Saraf,Langmuir20(13),5539-5543 (2004).
22 Z. Li, G. Luppi, A. Geiger, H. P. Josel, and L. De Cola, Small 7(22), 3193-3201 (2011).
23 M. Cretich, V. Sedini, F. Damin, M. Pelliccia, L. Sola and M. Chiari, Analytical biochemistry 397(1), 84-88 (2010).
24 Y. Okahata, M. Kawase, K. Niikura, F. Ohtake, H. Furu- sawa, and Y. Ebara, Analytical Chemistry 70(7), 1288-1296 (1998).
25 E. Özumur, S. Ahn, A. Yalçın, C.A.Lopez, E. Çevik, R.J. Irani, C. DeLisi, M. Chiari and M.S. Ünlü, Biosensors and Bioelectronics 25(7), 1789-1795 (2010).

6.2 Conference Paper

26 K. B. Gylfason, B. Sánchez, A. Griol, C. A. Barrios, H. Sohlström, R. Casquel, D. Hill, and G. Stemme, Robust hybridization of nanostructured buried integrated optical waveguide systems with on-chip fluid handling for chemical analysis, in: Micro Total Analysis Systems (mu- TAS). Enschede, The Netherlands. 14-18 May 2000, (2008), pp. 399-401.

7 Appendices

7.1 Microring Fabrication Procedure

The microchip are made in Universitat Politecnica De Valencia. A 300 nm Silicon Nitride layer is deposited over Silica-over-Silicon wafer by PECVD. A photo-mask aligner was used to make the photolithography process using UV AZ-MIR701 resist. This resist served to make a lift-off of a chromium layer evaporated by an electron beam physical vapour deposition and was removed by a high pressure jet of solvent (NMP). The chromium layer was used as a mask to transfer the waveguide structures in the 300 nm thick nitride by etching using ICP plasma etcher with CF_4. This chromium mask was then removed in a chromium etchant (CR-7) followed by a piranha cleaning. Following the procedure presented by K.B. Gylfason[26], a new layer of chromium was deposited over the sensing microrings that would be used as sensors with a second level of mask aligner lithography by lift-off process using once again the AZ-MIR701 resist. The cladding layer of silica was deposited by PECVD on top of the wafer and then removed only over the sensing microrings by ICP etching using a mixture of CF_4 and C_4F_8. This layer of Cr was used as a protection layer to prevent etching the nitride structures while etching the cladding silica layer. CR-7 etchant was used to remove this protection layer (followed by a piranha cleaning). Wafer was then diced in several $1\ cm^2$ chips, that have been tested to verify their working condition.

7.2 Materials

Polydimethylsiloxane SYLGARD 184 (PDMS elastomer kit) was purchased from Dow Corning (Midland, MI, USA). Hydrochloric acid, hydrogen peroxide, sodium bicarbonate, ethanolamine, (3-Aminopropyl)triethoxysilane (APTES), N-(3-Dimethylaminopropyl)-N'-ethylcarbodiimide (EDC), isopropanol, SSC (saline sodium citrate), SDS (Sodium dodecyl sulfate) and BSA (Bovine Serum Albumin) were supplied by Sigma Aldrich. DNA strands were supplied by Metabion (Germany).